

Accepted Manuscript

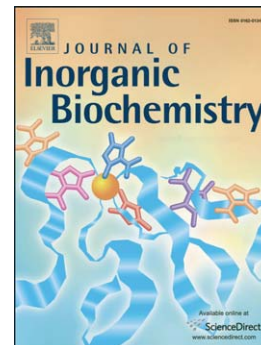
Neomycin B-cyclen conjugates and their Zn(II) complexes as RNA binding agents

Bopha Kong, Tanmaya Joshi, Matthew J. Belousoff, Yitzhak Tor, Bim Graham, Leone Spiccia

PII: S0162-0134(15)30130-6
DOI: doi: [10.1016/j.jinorgbio.2015.11.029](https://doi.org/10.1016/j.jinorgbio.2015.11.029)
Reference: JIB 9860

To appear in: *Journal of Inorganic Biochemistry*

Received date: 1 October 2015
Revised date: 9 November 2015
Accepted date: 30 November 2015



Please cite this article as: Bopha Kong, Tanmaya Joshi, Matthew J. Belousoff, Yitzhak Tor, Bim Graham, Leone Spiccia, Neomycin B-cyclen conjugates and their Zn(II) complexes as RNA binding agents, *Journal of Inorganic Biochemistry* (2015), doi: [10.1016/j.jinorgbio.2015.11.029](https://doi.org/10.1016/j.jinorgbio.2015.11.029)

This is a PDF file of an unedited manuscript that has been accepted for publication. As a service to our customers we are providing this early version of the manuscript. The manuscript will undergo copyediting, typesetting, and review of the resulting proof before it is published in its final form. Please note that during the production process errors may be discovered which could affect the content, and all legal disclaimers that apply to the journal pertain.

Neomycin B-Cyclen Conjugates and their Zn(II) Complexes as RNA Binding Agents

Bopha Kong,^a Tanmaya Joshi,^{a} Matthew J. Belousoff,^b Yitzhak Tor,^c Bim Graham,^{d*} and Leone
Spiccia^{a*}*

- a) School of Chemistry, Monash University, Victoria 3800, Australia.
b) Department of Microbiology, Monash University, Victoria 3800, Australia.
c) Department of Chemistry and Biochemistry, University of California, San Diego, 9500 Gilman Drive, La Jolla, CA, 92093-0332, USA.
d) Monash Institute of Pharmaceutical Sciences, Monash University, Parkville, Vic 3052, Australia.

*“In memory of Professor Graeme Hanson and his contributions to Bioinorganic Chemistry and
Electron Paramagnetic Resonance”*

*Corresponding authors:

tanmaya.joshi@monash.edu; bim.graham@monash.edu; leone.spiccia@monash.edu.

Fax: +61 3 9905 4597 (T.J. and L.S.); +61 3 9903 9582 (B.G.)

Key words: aminoglycoside derivatives, antibiotics, 1,4,7,10-tetraazacyclodecane, RNA, zinc(II) complexes

Abstract

Three new conjugates featuring the aminoglycoside antibiotic neomycin B linked to the 1,4,7,10-tetraazacyclododecane (cyclen) macrocycle via alkyl chains of varying lengths were synthesized from suitably protected derivatives of these precursors via conventional peptide coupling protocols. The final products were characterized by ^1H NMR spectroscopy, mass spectrometry, and elemental analysis. FRET-based measurements examining the ability of the compounds to displace coumarin-labelled kanamycin A or neomycin B from Dy547-labelled prokaryotic ribosomal A-site RNA revealed that they bind to the A-site with slightly higher affinities than the parent aminoglycoside (e.g., IC_{50} at pH 7 = 1.42–2.30 μM vs. 2.35 μM for neomycin B). This is attributed to the higher overall positive charge of the conjugates, resulting from protonation of the macrocyclic amines. Consistent with a predominantly electrostatic mode of interaction, the binding affinities of the conjugates were found to increase with decreasing pH, reflecting a greater degree of protonation at lower pH. The zinc(II) complexes of the neomycin B-cyclen conjugates were found to bind to A-site RNA with even higher affinities (IC_{50} = 0.85–1.32 μM), due to the Zn(II)-cyclen motif forming coordinative (and/or electrostatic) interactions with the uracil bases and/or phosphate groups within the A-site. These results highlight the potential for the nucleic acid-binding properties of aminoglycosides to be tuned via the covalent attachment of metal complexes, which could ultimately prove useful to the development of new anti-bacterial and anti-viral agents.

Introduction

Aminoglycosides are naturally occurring compounds that consist of an aminocyclitol ring linked to aminosugars.¹ The discovery of the antibiotic activity of these compounds and the seminal findings on their interactions with RNA have together opened up new avenues in the design of small molecule-based RNA-targeting therapeutics.¹⁻¹¹ Because of their polycationic nature (arising from the presence of multiple protonated amine groups), combined with the conformational “plasticity” of RNA, the aminoglycosides are fairly promiscuous RNA binders.¹² Their bactericidal activity, primarily limited to aerobic Gram-negative bacteria, derives from their ability to bind to the so-called “A-site” of the decoding region (i.e., the site of codon-anticodon recognition) of bacterial 16S ribosomal RNA within the 30S ribosomal subunit (Figure 1), which leads to a loss of translational fidelity during protein synthesis.^{2, 13-15} However, studies have shown that aminoglycosides can also bind to a number of RNA targets with high affinity, including group I introns and the hammerhead, hairpin and hepatitis delta virus ribozymes.² Of perhaps greatest interest, several aminoglycosides bind to a number of RNA motifs found within the HIV-1 genome, namely loops of the HIV-1 dimerisation initiation site (DIS),¹⁶ the junction of HIV-1 rev response element (RRE)¹⁷ and the major groove of the HIV-1 transactivation response element (TAR),¹⁸⁻²¹ indicating that there is scope to develop aminoglycoside-based anti-viral agents.

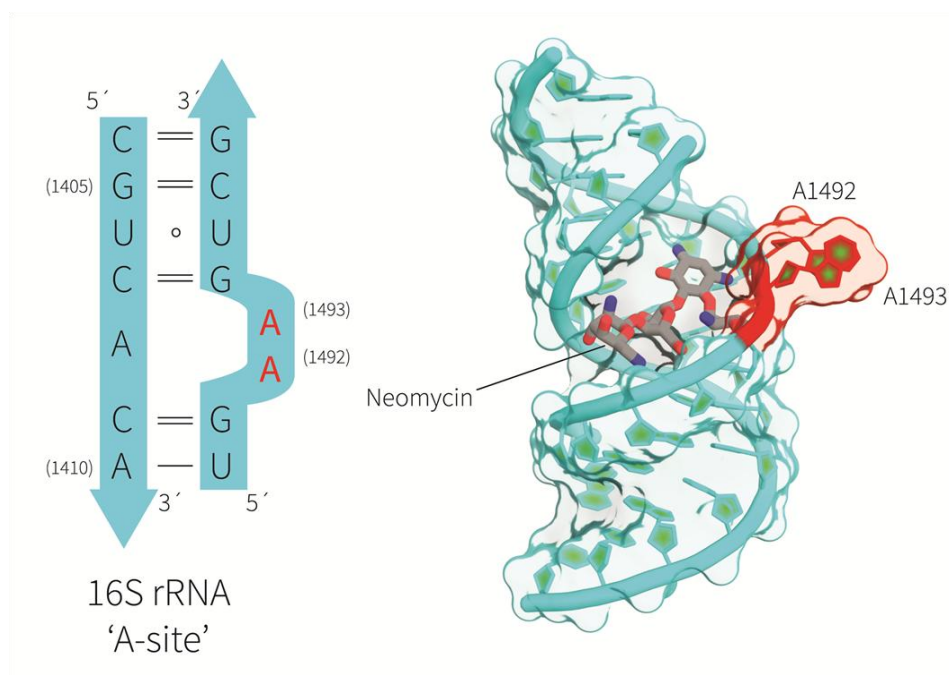


Figure 1. Structure of the 16S prokaryotic ribosomal A-site (left, the binding site of the aminoglycoside Neomycin B shown in red)²² and (right) Neomycin B binding to a 16S prokaryotic ribosomal construct (PDB entry: 2A04,¹² graphic prepared using PyMOL).

The widespread use of aminoglycosides as antibiotic drugs has been compromised by their toxicity and the emergence of bacterial resistance.^{4-7, 9-10} As a result, synthetic modifications to aminoglycosides have been investigated in an attempt to produce derivatives that not only display higher affinities and selectivity for specific therapeutically-significant RNA motifs, but which are also less prone to metabolic alterations by aminoglycoside-modifying enzymes.^{4-7, 9-10, 23} By way of example, conjugation of chloramphenicol and linezolid to the aminoglycoside, neomycin B, enhances the binding affinity for HIV-1 TAR by approximately 10-fold relative to the parent aminoglycoside (Figure 2).²⁴ A library of neomycin-dipeptide conjugates with enhanced HIV-1 RRE binding affinities have also been developed.²⁵ To date, one of the strongest competitive inhibitors of the interaction between RRE and its cognate binding partner, the rev protein, is a neomycin-acridine conjugate (**Neo B-acridine**, Figure 2) that exhibits an affinity for RRE similar to that of rev itself.¹⁷

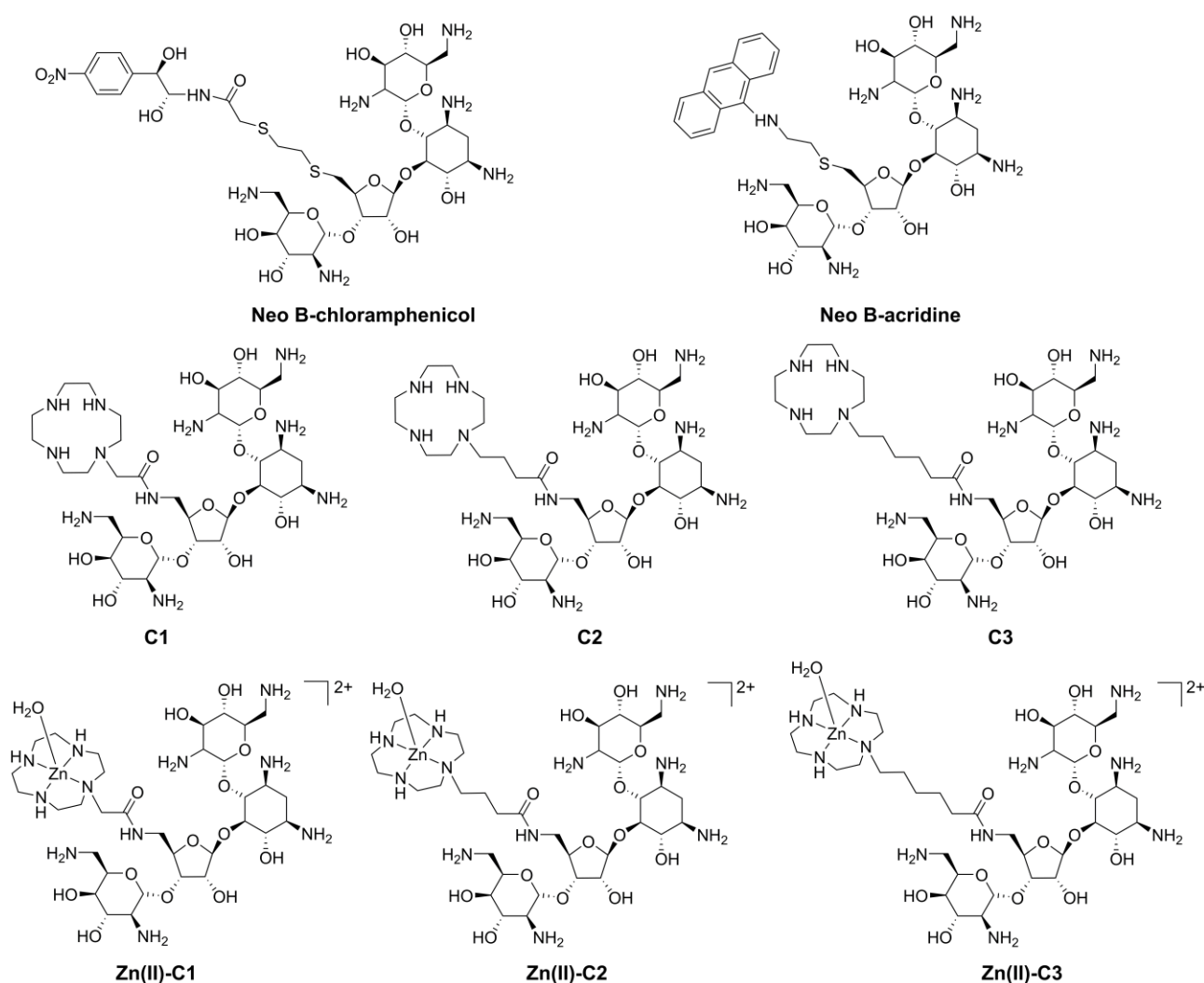


Figure 2. Structures of the reported RNA-binding neomycin B conjugates, **Neo B-chloramphenicol** and **Neo B-acridine**, and the neomycin B-cyclen conjugates, **C1–C3** and Zn(II)-C1–Zn(II)-C3, developed in this study.

Herein, we describe the synthesis and A-site binding properties of a series of new neomycin B conjugates featuring the polyazamacrocycle, 1,4,7,10-tetraazacyclododecane (cyclen) appended to their D-ribose ring, as well as the corresponding Zn(II) complexes (**C1–C3** and Zn(II)-C1–Zn(II)-C3, Figure 2). Given that previous studies have shown that the high affinity of aminoglycosides for RNA is associated predominantly with the formation of complementary electrostatic interactions between protonated amine groups on the aminoglycosides and the polyanionic sugar-phosphate backbone of RNA,^{3, 12, 26-27} it was hypothesised that the tethered cyclen macrocycle, with its additional ionisable amino groups, might enhance affinity for the A-site RNA motif. Additionally, we assessed whether

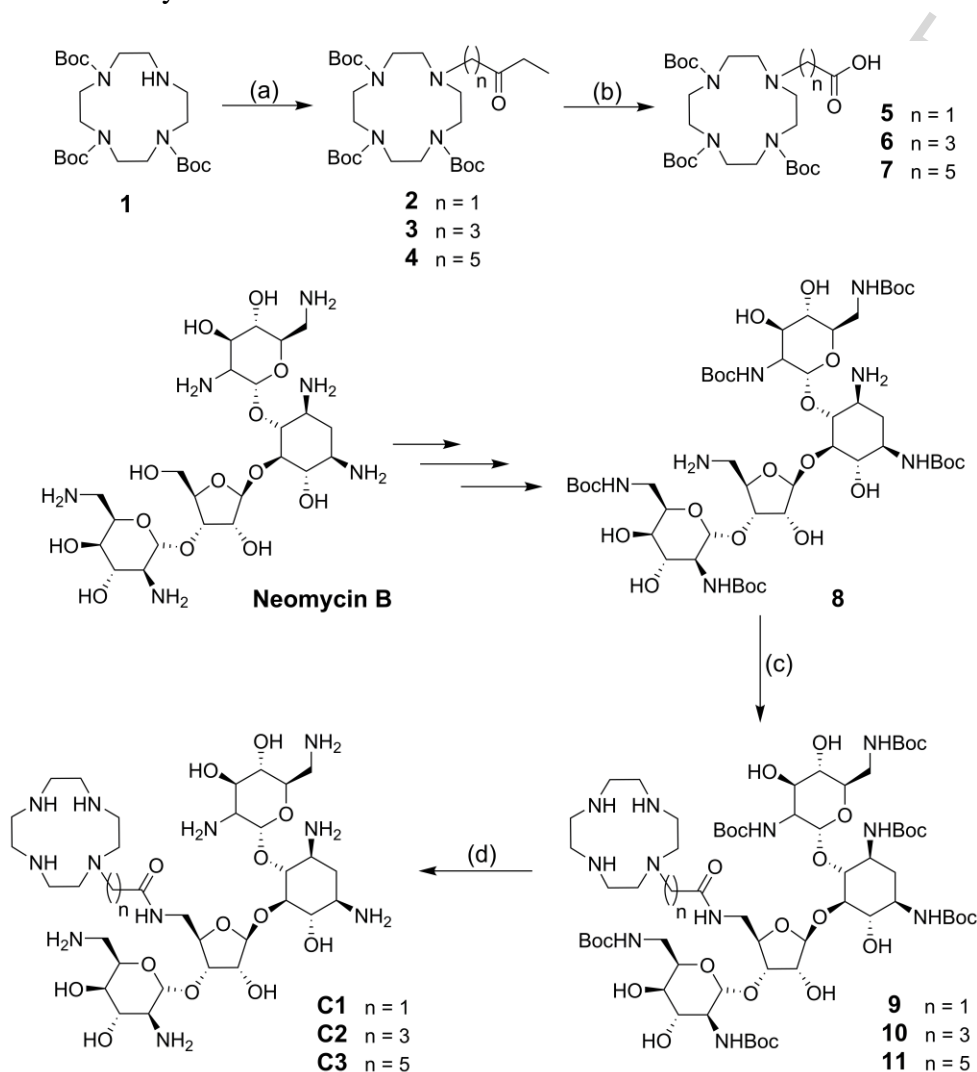
complexation of Zn(II) by cyclen might serve to enhance the affinity still further by allowing the conjugates to form coordination bonds with the RNA target. Previous studies have shown that Zn(II)-cyclen complexes form reasonably strong interactions with phosphate groups as well as the deprotonated imide groups of the nucleobases, uracil and thymine.²⁸⁻³¹

Results and Discussion

Synthesis of neomycin B-cyclen conjugates. A convergent synthetic approach was used to access the conjugates (Scheme 1). Firstly, Boc-protected cyclen derivatives incorporating a single carboxylic acid pendant arm (**5–7**), as well as a Boc-protected neomycin B derivative featuring a solitary free amino group at the 5'' position of the central D-ribose ring (**8**), were prepared and characterized by ¹H NMR and IR spectroscopy, and mass spectrometry. These two components were then linked together under standard HBTU/HOBt-mediated amide coupling conditions. Following purification by silica gel column chromatography, the Boc-protected forms of the desired conjugates (**9–11**) were isolated in good yield (70–85%) and high purity. The ¹H NMR spectra showed numerous resonances in the aliphatic region (1.0–6.0 ppm) characteristic of neomycin B, with additional signals in the upper field region ascribed to alkyl CH₂ protons. The appearance of additional broad singlet and multiplets between δ 2.0–4.0 ppm were attributed to the CH₂ protons of the cyclen ring. The ¹³C NMR spectra of **9–11** each showed a signal between δ 170.5–170.9 ppm, corresponding to an amide C=O and confirming successful amide coupling of **5–7** to **8**. Formation of **9–11** was further corroborated by the presence of the expected parent [M+H]⁺ signals at m/z = 1727.9, 1754.5 and 1784.0, respectively, in the low-resolution electrospray ionization (ESI) mass spectrum.

Following trifluoroacetic acid (TFA)-mediated removal of the Boc groups and subsequent preparative RP-HPLC purification, the final conjugates, **C1–C3** (Figure 2), were obtained in high purity, albeit in low yield (35–40%). The identity of the conjugates was confirmed by high-resolution

ESI MS analysis, with parent $[M+H]^+$ signals observed at $m/z = 826.4998$, 854.5283 , 882.5649 for **C1**, **C2** and **C3**, respectively. The protonation state and number of TFA counterions was established by elemental analysis.



Scheme 1. Synthesis of neomycin-cyclen conjugates, **C1–C3**. *Reagents and conditions:* (a) ethyl ω -bromoalkanoate, K_2CO_3 , CH_3CN , Δ , 48–72 h, 73–85%; (b) 1 M NaOH, EtOH, rt, 15 h, ca. 90%; (c) cyclen carboxylic acids **5–7**, HBTU/HOBt, DIPEA, dry CH_2Cl_2 , rt, 20 h, 72–82%; (d) TFA/ CH_2Cl_2 (1:1), rt, 5 h.

Displacement binding studies. Displacement binding of the RNA targets was probed using the Dy547-labelled RNA/coumarin-labelled aminoglycoside system previously described by Tor *et al.*³²⁻³³ Figure 3 illustrates the working concept for this FRET-based displacement binding assay. When the aminoglycoside-coumarin is photoexcited, energy is transferred to the Dy547 dye. Energy transfer

manifests itself as quenching of the coumarin fluorescence and a reduction of the excited state lifetime, accompanied by an increase in fluorescence emission from the nearby Dy547 molecule. The binding affinity of a test compound can be established by adding it in increasing concentration to the pre-formed FRET complex and measuring the accompanying fluorescence changes. Gradual displacement of the RNA-bound aminoglycoside-coumarin by the test compound results in the coumarin and Dy547 no longer being close enough for FRET to occur, leading to an increase in observed fluorescence emission from the coumarin and a decrease in that from Dy547.³²⁻³³

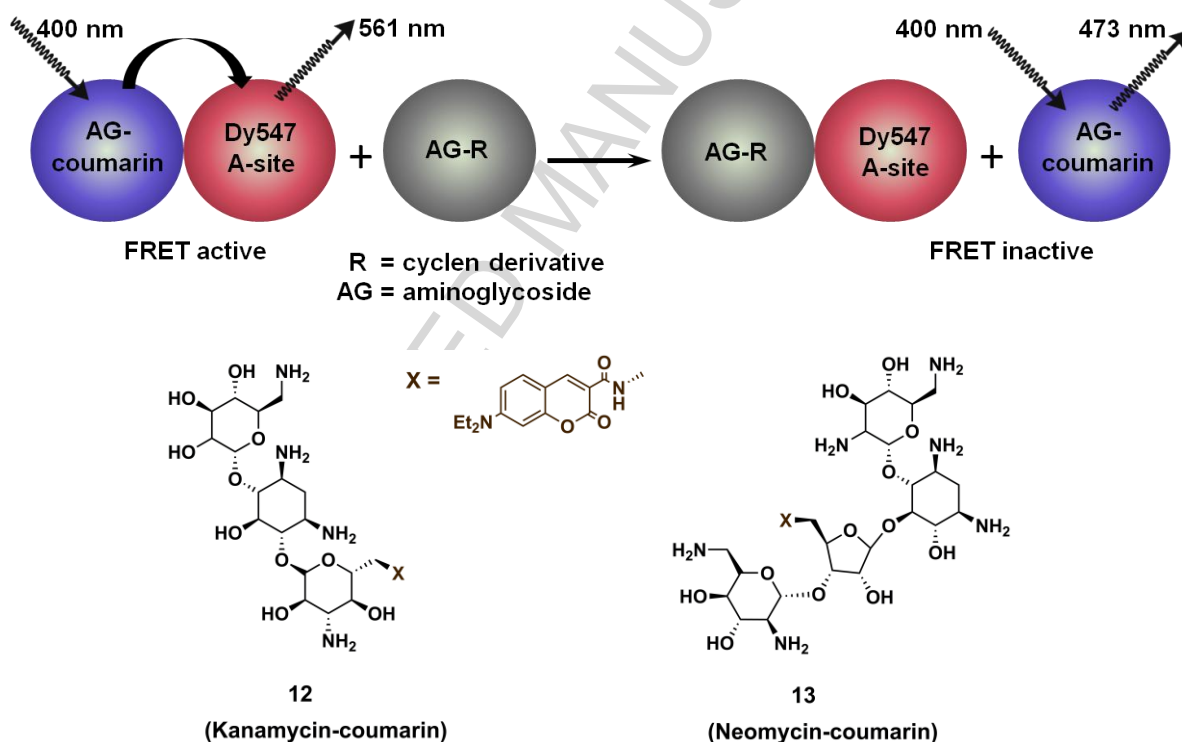


Figure 3. FRET-based displacement-style assay for determining A-site binding affinity. *Conditions:* $\lambda_{\text{ex}} = 400 \text{ nm}$, $\lambda_{\text{em}} = 473 \text{ nm}$ (coumarin) and 561 nm (Dy547).³²⁻³³

In this work, either kanamycin A- or neomycin B-coumarin (donor) was used in combination with the Dy547 A-site RNA (acceptor). As expected, titration of **C1–C3** and their corresponding Zn(II) complexes, Zn(II)-**C1–Zn(II)-C3**, into this FRET-active system resulted in an increase in the coumarin emission (473 nm) and a concurrent reduction in Dy547 emission (561 nm) when excited at 400 nm (see Figure S1 for a representative titration dataset). Plotting of the fractional fluorescence saturation at

561 nm against the concentration of the test compound yielded displacement curves (see Figure S2 for the corresponding dose response curve), from which the 50% inhibition concentration (IC_{50}) values were calculated (see experimental section for more details).

Figure 4 shows the dose response curves for the displacement of kanamycin A-coumarin from Dy547 A-site by neomycin B and the conjugates **C1–C3**, with the corresponding IC_{50} values presented in Table 1. Compared to neomycin B ($IC_{50} = 0.68 \pm 0.09 \mu\text{M}$), the conjugates exhibit slightly higher affinity for the A-site ($IC_{50} = (0.51 \pm 0.06)$ to $(0.31 \pm 0.10) \mu\text{M}$).

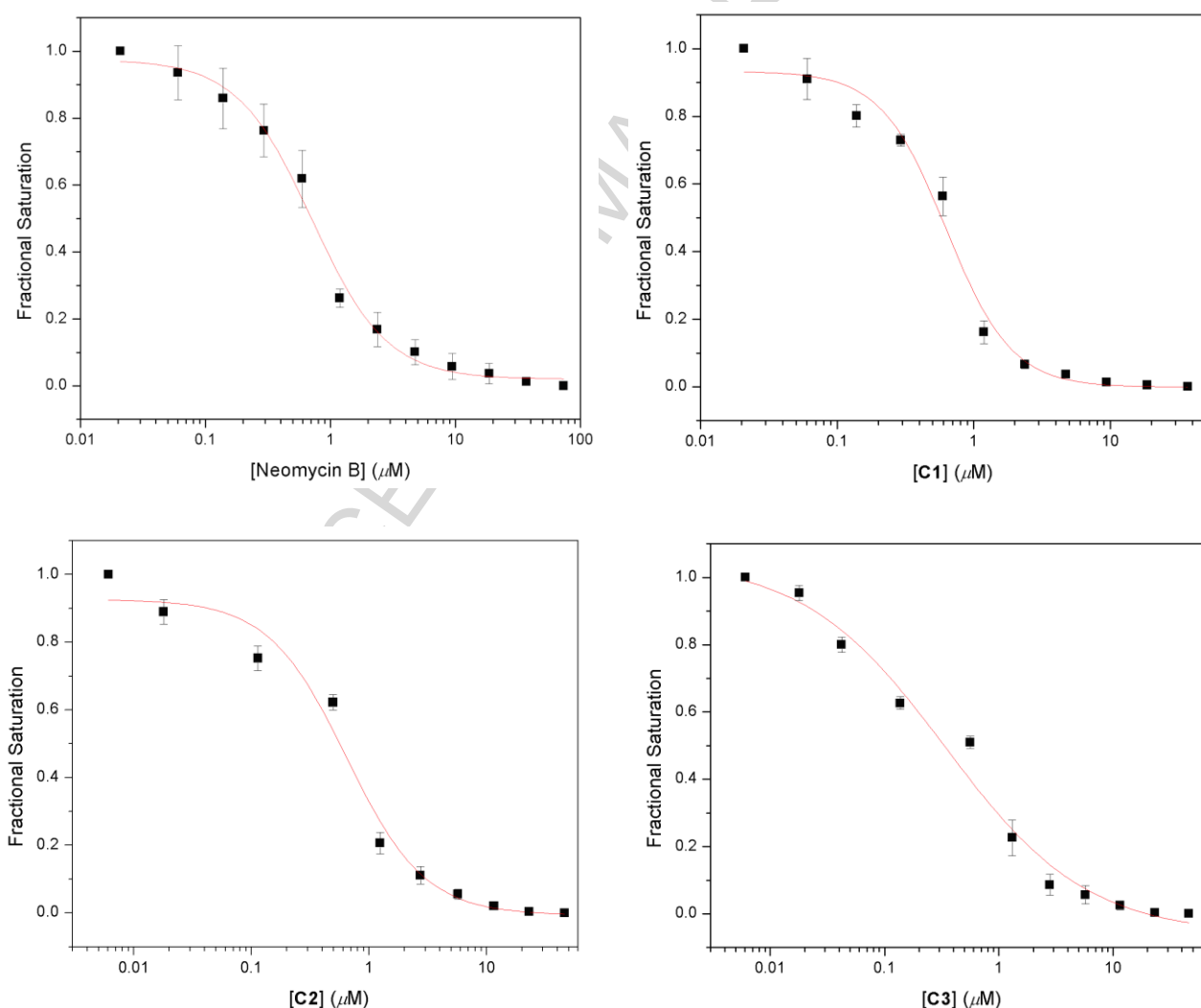


Figure 4. Dose response curves (measured at 561 nm) for the displacement of kanamycin A-coumarin from the Dy547 A-site by neomycin B and conjugates **C1–C3**. *Conditions:* [Dy547 A-site] = 1 μM , [kanamycin A-coumarin] = 0.5 μM , [cacodylate] = 20 mM, (pH = 7.0 @ 21 °C), [NaCl] = 100 mM, [EDTA] = 0.5 mM.

Table 1. IC₅₀ values for the displacement of kanamycin A-coumarin from the Dy547 A-site by neomycin B and the conjugates **C1–C3**.

Conjugate	IC ₅₀ (μM)
C1	0.51 ± 0.10
C2	0.45 ± 0.08
C3	0.31 ± 0.05
Neomycin B (control)	0.68 ± 0.09

Conditions: [Dy547 A-site] = 1 μM, [kanamycin A-coumarin] = 0.5 μM, [cacodylate] = 20 mM, (pH = 7.0 @ 21 °C), [NaCl] = 100 mM, [EDTA] = 0.5 mM. Values represent the mean ± SD of 3 experiments.

The degree of protonation (and hence average overall charge) of the kanamycin A and neomycin B derivatives is expected to vary significantly with pH. Thus, the strength of binding between the kanamycin A-coumarin/neomycin B derivatives and the target A-site will be dependent on pH. The affinity of neomycin B itself for the bacterial A-site has previously been found to be pH dependent.³⁴ For the neomycin B derivatives, protonation of amino groups would see the neomycin B moiety existing predominantly in the 5+ protonation state, and cyclen in the 2+ protonation state, at physiological pH.^{27, 35-36} Introduction of cyclen is thus expected to increase the overall positive charge of the conjugates, and enhance their electrostatic interactions (charge-assisted hydrogen bonding interactions) with the negatively charged A-site. It should be noted that any given pH, both the kanamycin A-coumarin and neomycin B derivatives will exist as a mixture of species with different protonation states, with the measured displacement constant (IC₅₀ value) representing the overall average contribution of all species present.

With the above in mind, we further examined how the additional amino groups present in cyclen might influence the binding event. Previously, it was noted that conjugate **C1**, which has an ethyl spacer between the neomycin B and cyclen, has the lowest binding affinity for the A-site (see Table 1). Thus, **C1** along and neomycin B were further tested to see if binding affinity could be improved under different pH conditions. Figures S3 and S4 (Supporting Information) illustrate the

displacement plots for neomycin B and **C1** at pH values between 6.0–8.5, with the corresponding IC_{50} values presented in Table 2.

Table 2. IC_{50} values for the displacement of kanamycin A-coumarin from Dy547 A-site by **C1** and neomycin B at pH 6.0–8.5.

pH	C1 IC_{50} (μ M)	Neomycin B IC_{50} (μ M)
6.0	0.35 ± 0.09	0.63 ± 0.09
6.5	0.42 ± 0.01	0.65 ± 0.07
7.0	0.51 ± 0.09	0.68 ± 0.10
7.5	0.61 ± 0.08	0.73 ± 0.07
8.0	0.72 ± 0.01	0.85 ± 0.05
8.5	0.88 ± 0.08	1.20 ± 0.07

Conditions: [Dy547 A-site] = 1 μ M, [kanamycin A-coumarin] = 0.5 μ M, [cacodylate] = 20 mM, (pH = 6.0–8.5 @ 21 °C), [NaCl] = 100 mM, [EDTA] = 0.5 mM. Values represent the mean \pm SD of 3 experiments.

The strength of the interaction between **C1** and the Dy547 A-site was found to steadily increase with decreasing pH (see also Figure 5); the IC_{50} for **C1** decreased by up to 0.2 μ M per unit decrease in pH (0.35–0.88 μ M for pH 6.0–8.5). Binding of neomycin B was also strongest at lower pH, but below pH 7.5 the IC_{50} values decreased only slightly with further reductions in pH. Overall, the fact that, at each tested pH, **C1** exhibited lower IC_{50} values than neomycin B indicates that **C1** is a better A-site binder compared to unmodified neomycin B. We postulate that the additional cationic charge introduced into **C1–C3** by the amino groups present on the cyclen macrocycle helps to promote the displacement of kanamycin A-coumarin from the A-site, thereby resulting in a marginal improvement in binding ability. The length of the carbon spacer between neomycin B and cyclen in the conjugate did not have much of an effect on the strength of binding.

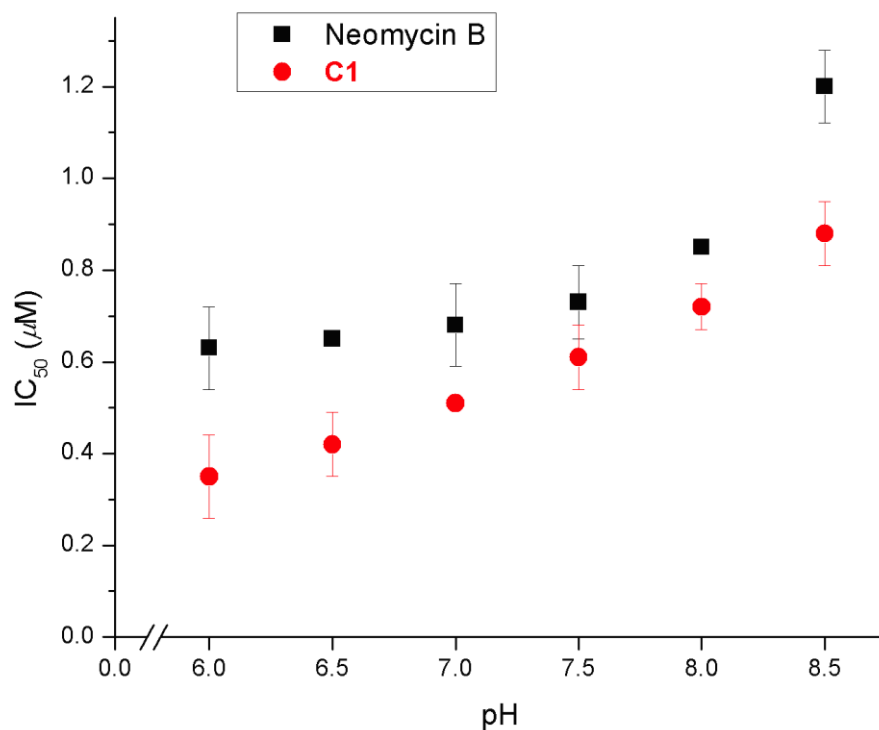


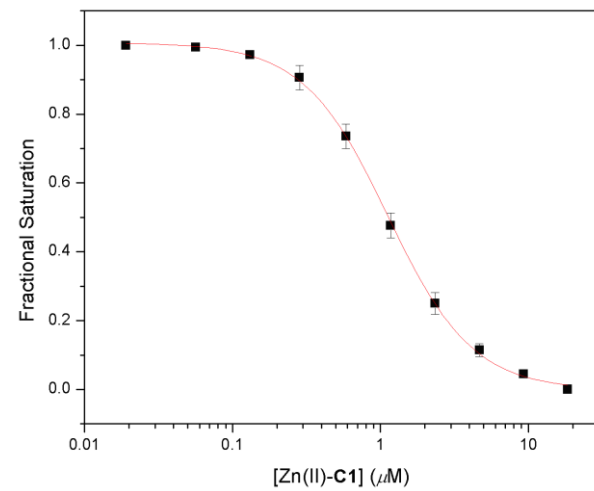
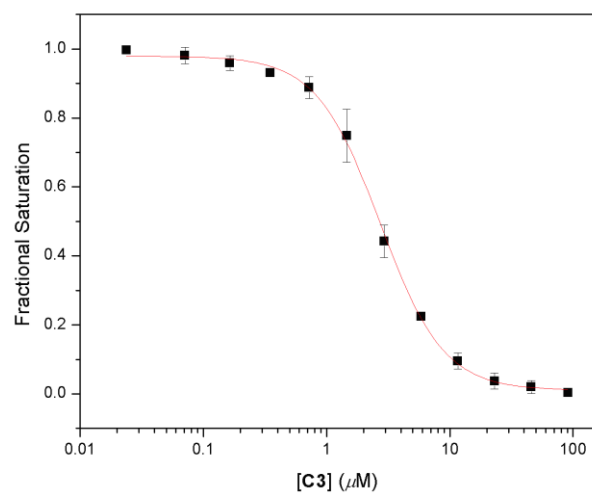
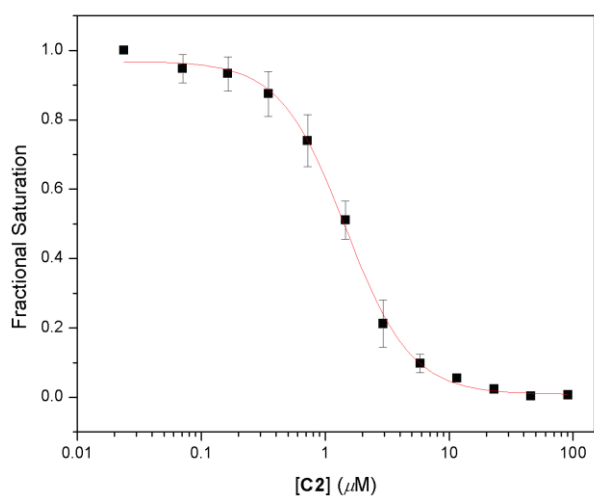
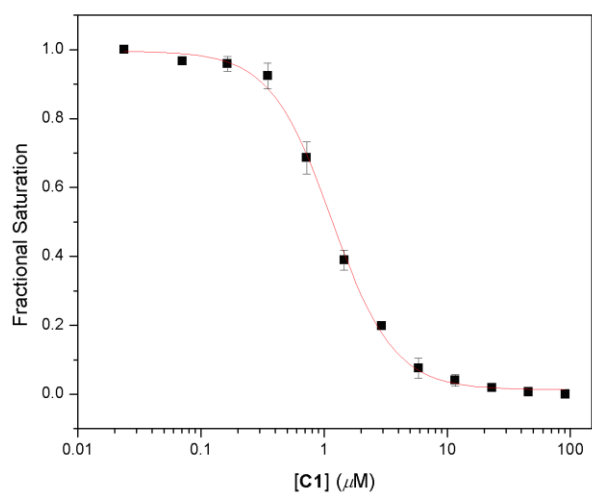
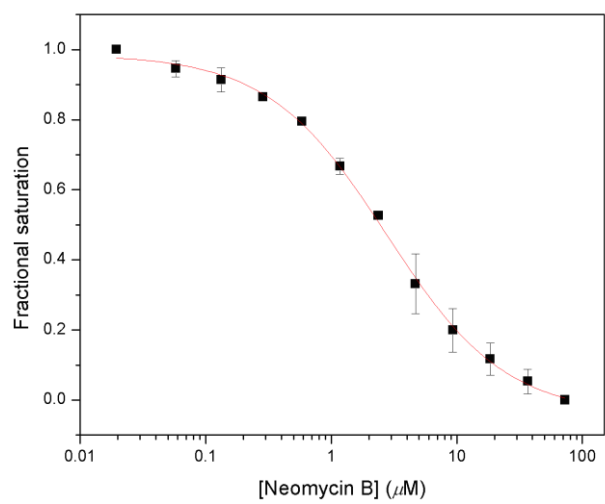
Figure 5. Plot of the variation in IC_{50} values (μM) with pH for **C1** and neomycin B. *Conditions:* [Dy547 A-site] = 1 μM , [kanamycin A-coumarin] = 0.5 μM , [cacodylate] = 20 mM, (pH = 6.0–8.5 @ 21 °C), [NaCl] = 100 mM, [EDTA] = 0.5 mM.

Further studies were conducted to investigate if the conjugates can also displace the stronger aminoglycoside A-site binder, neomycin B-coumarin.³²⁻³³ Figure 6 shows the displacement plots for **C1–C3** and Zn(II)-**C1–Zn(II)-C3**, with the corresponding IC_{50} values presented in Table 3.

Table 3. IC_{50} values for the displacement of neomycin B-coumarin from Dy547 A-site by **C1–C3** and the corresponding Zn(II) metal complexes.

Conjugate	IC_{50} (μM)	Complex	IC_{50} (μM)
C1	1.77 ± 0.09	Zn(II)- C1	1.13 ± 0.09
C2	1.42 ± 0.26	Zn(II)- C2	1.32 ± 0.19
C3	2.30 ± 0.22	Zn(II)- C3	0.85 ± 0.04
Neomycin B	2.35 ± 0.31		

Conditions: [Dy547 A-site] = 1 μM , [neomycin B-coumarin] = 0.5 μM , [cacodylate] = 20 mM, (pH = 7.0 @ 21 °C), [NaCl] = 100 mM, [EDTA] = 0.5 mM (no EDTA for metal complex titration). Values represent the mean \pm SD of 3 experiments.



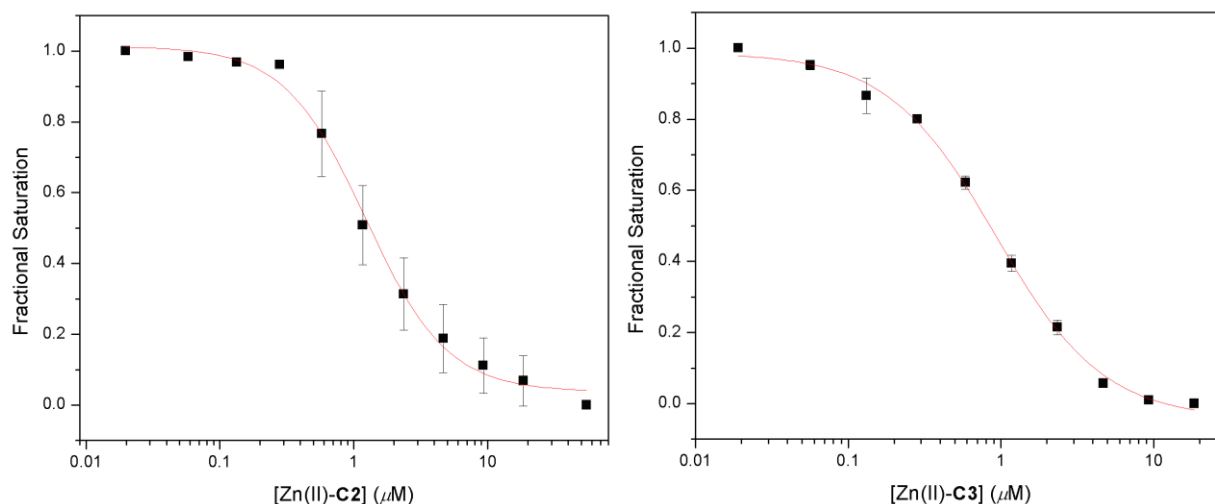


Figure 6. Displacement of neomycin B-coumarin from Dy547 A-site by neomycin B, **C1–C3**, and Zn(II)-**C1–Zn(II)-C3**. Conditions: [Dy547 A-site] = 1 μM , [neomycin B-coumarin] = 0.5 μM , [cacodylate] = 20 mM, (pH = 7.0 @ 21 $^{\circ}\text{C}$), [NaCl] = 100 mM, [EDTA] = 0.5 mM (no EDTA for metal complex titration).

As expected, larger IC_{50} values were obtained, since neomycin B-coumarin is harder to displace from the A-site.³²⁻³³ The addition of Zn(II) ion to **C1–C3** enhanced their affinity for the A-site, but to varying degrees; Zn(II)-**C2** showed only marginally improved affinity, while Zn(II)-**C3** bound the A site two-fold more strongly than its non-metallated counterpart. This is consistent with the fact that anionic phosphates,²⁹⁻³¹ and uracil and thymine bases in RNA and DNA, respectively,²⁸⁻³⁰ bind strongly to Zn(II)-cyclen motifs via coordinative and/or electrostatic interactions. The presence of uracil bases near the aminoglycoside binding site (Figure 1) may explain the enhanced binding affinities of the Zn(II)-loaded neomycin B conjugates. The high affinity of Zn(II)-**C3** for the A-site may stem from the fact that this conjugate includes the longest carbon spacer, which might allow the Zn-cyclen moiety to better position itself to bind to a uracil base.

Of note, in our case, a lower IC_{50} value was obtained for the displacement of neomycin B-coumarin by neomycin B ($2.35 \pm 0.31 \mu\text{M}$) compared to the reported value of $4.4 \pm 0.3 \mu\text{M}$.²³

Conclusion

Three new neomycin B-cyclen conjugates have been developed that exhibit higher affinities for the bacterial ribosomal A-site than neomycin B itself, with IC_{50} values lying in the sub-micromolar-to-micromolar range. We attribute the stronger binding to the increased overall positive charge of the conjugates arising from the presence of the protonated cyclen ring. The A-site affinities of each of the compounds was found to be dependent on pH and, therefore, by implication, their protonation state – the lower the pH (higher the charge), the higher the affinity for the A-site. The Zn(II) complexes of the conjugates bound to the A-site even more strongly than the conjugates, which may be due to the cationic Zn(II)-cyclen moiety forming coordinative (and/or electrostatic) interactions with the phosphates or deprotonated uracil bases present within the A-site. We are currently investigating the ability of the conjugates and their Zn(II) complexes to hydrolytically-cleave selected bonds within the A-site, as well as their affinity towards other (potentially) therapeutically-relevant RNA targets, in particular the HIV-1 TAR, RRE and DIS motifs.

Experimental Section

Materials. All chemicals were of reagent grade quality or better, obtained from commercial suppliers and used without further purification. Solvents were used as received or distilled using standard procedures. Deionised water was used for all reactions in aqueous solution. *Column chromatography* was performed using Silica gel 60 (0.040–0.063 mm mesh, Merck). The Dy547-labelled A-site RNA oligonucleotide (deprotected and purified) was purchased from Dharmacon. Standard $ZnCl_2$ solution was purchased from Merck. Chemicals for preparing buffer solutions were purchased from Sigma-Aldrich (enzyme free-grade). Autoclaved water was used for all fluorescence titrations.

Instrumentation and methods. 1H and ^{13}C NMR spectra were recorded in deuterated solvents at room temperature on either Bruker spectrometers (AC 200, AM 300, Avance DR 400) or Varian

Spectrometers (Mercury 300 and 500). The chemical shifts, δ , are reported in ppm (parts per million). The signals from the residual protons of deuterated solvent were used as an internal reference. The abbreviations for the peak multiplicities are as follows: s (singlet), d (doublet), dd (doublet of doublets), t (triplet), q (quartet), m (multiplet), and br (broad). *ESI mass spectrometry* was performed on a Micromass Platform II Quadrupole Mass Spectrometer fitted with an electrospray source. The capillary voltage was 3.5 eV and the cone voltage was 3.5 eV. *High-resolution mass spectra* were recorded with a Bruker BioApex II 47e FT-ICR MS fitted with an Analytica Electrospray Source. Samples were introduced via a syringe pump at a rate of $1 \mu\text{L min}^{-1}$ and the capillary voltage was set at 200 V. *Infrared spectra* were recorded on neat samples at a resolution of 4.0 cm^{-1} using an Agilent Technologies Cary 630 FTIR (ATR) or a Perkin-Elmer FTIR 1600 series spectrometer. Peak intensities are given as broad (br), very strong (vs), strong (s), medium (m) and weak (w). *Reverse phase-HPLC analyses* were performed using a Jupiter C18 Column ($5 \mu\text{m}$ particle size, 300 \AA pore size, $4.6 \times 250 \text{ mm}$). Solution A consisted of 0.1% TFA in water and solution B of 0.1% TFA in MeCN. Chromatographic separations were performed used a gradient from 0–100% B over 40 min, with a flow rate of 1 mL min^{-1} and UV detection at $\lambda = 210 \text{ nm}$. *Microanalyses* were carried out by the Campbell Microanalytical Laboratory, University of Otago, New Zealand.

Syntheses. The compounds 1,4,7-*tris*(*tert*-butoxycarbonyl)-1,4,7,10-tetraazacyclododecane (**1**),³⁷ 5'-Amino-*N*-Boc-protected neomycin B (**8**),³ kanamycin A-coumarin (**12**)³²⁻³³ and neomycin B-coumarin (**13**)³²⁻³³ were synthesised according to literature procedures, with all characterisation data in agreement with that reported previously.

1-(2-(Ethoxycarbonyl)ethyl)-4,7,10-tris(tert-butoxycarbonyl)-1,4,7,10-tetraazacyclododecane (**2**). To a stirred mixture of compound **1** (1.03 g, 2.2 mmol) and anhydrous K_2CO_3 (1.78 g, 13 mmol) in CH_3CN (15 mL) was added ethyl bromoacetate (0.35 mL, 3.1 mmol) in CH_3CN (15 mL) in a dropwise fashion. The mixture was then heated to reflux. After 48 h, the reaction mixture was cooled to room temperature, filtered and the solvent removed under reduced pressure to afford **2** as a yellow oil, which

was purified *via* column chromatography (eluent: *n*-hexane/EtOAc, 2:1 v/v) ($R_f = 0.47$). Yield: 0.75 g (85%). ^1H NMR (500 MHz, CDCl_3) δ (ppm): 1.12 (t, 3H, $J = 7.0$ Hz, ethyl CH_3), 1.30 (s, 27H, ^tBu CH_3), 2.76–2.79 (m, 4H, cyclen ring CH_2), 3.19–3.27 (m, 8H, cyclen ring CH_2), 3.35–3.42 (m, 8H, cyclen ring CH_2 and acetate CH_2), 4.06 (q, 2H, $J = 7.0$ Hz, ethyl CH_2). ^{13}C NMR (125 MHz, CDCl_3) δ (ppm): 14.3 (ethyl CH_3), 28.5 (^tBu CH_3), 47.1, 47.4, 47.7, 50.0, 51.2, 53.5 (cyclen CH_2), 54.9 (acetate CH_2), 60.3 (ethyl CH_2), 79.5 (^tBu C), 155.3, 155.7, 156.1 (Boc group $\text{C}=\text{O}$), 170.6 (ester $\text{C}=\text{O}$). IR (cm^{-1}): 3363br w, 2979s, 2933s, 1736s, 1686s, 1461s, 1417s, 1367s, 1250s, 1162s, 1029m, 980m, 911m, 887w, 859m, 756s, 666m. ESI-MS (m/z): 559.2 $[\text{M}+\text{H}]^+$, 581.2 $[\text{M}+\text{Na}]^+$.

1-(4-(Ethoxycarbonyl)butyl)-4,7,10-tris(tert-butoxycarbonyl)-1,4,7,10-tetraazacyclododecane

(3). Compound **3** was synthesised from **1** (0.51 g, 1.1 mmol) and ethyl 4-bromobutyrate (0.43 g, 2.2 mmol) following the method described for compound **2**. The reaction mixture was refluxed for 72 h, and following work-up, **3** obtained as a yellow oil, which was purified *via* column chromatography (eluent: *n*-hexane/EtOAc, 2:1 v/v) ($R_f = 0.51$). Yield: 0.59 g (73%). ^1H NMR (500 MHz, CDCl_3) δ (ppm): 1.22 (t, 3H, $J = 7.5$ Hz, CH_3), 1.43 (s, 27H, ^tBu CH_3), 1.81–1.86 (m, 2H, butyl CH_2), 2.25 (t, 2H, $J = 4.0$ Hz, butyl CH_2), 2.39 (t, 2H, $J = 4.0$ Hz, butyl CH_2), 2.52–2.55 (m, 4H, cyclen ring CH_2), 3.2–3.45 (m, 8H, cyclen ring CH_2), 3.4–3.5 (m, 4H, cyclen ring CH_2), 4.10 (q, 2H, $J = 7.8$ Hz, ethyl CH_2). ^{13}C NMR (125 MHz, CDCl_3) δ (ppm): 14.5 (ethyl CH_3), 24.1 (butyl CH_2), 28.5 (^tBu CH_3), 31.8 (butyl CH_2), 49.6, 50.6, 51.9, 52.3, 54.8, 55.5 (cyclen CH_2), 59.6 (butyl CH_2), 61.8 (ethyl CH_2), 79.9 (^tBu C), 155.7 (^tBu $\text{C}=\text{O}$), 173.3 (ester $\text{C}=\text{O}$). ESI-MS (m/z): 587.4 $[\text{M}+\text{H}]^+$ 609.3 $[\text{M}+\text{Na}]^+$.

1-(6-(Ethoxycarbonyl)hexyl)-4,7,10-tris(tert-butoxycarbonyl)-1,4,7,10-tetraazacyclododecane

(4). Compound **4** was synthesised from **1** (0.50 g, 1.1 mmol) and ethyl 6-bromohexanoate (0.47 g, 2.2 mmol) following the method described for compound **2**. The reaction mixture was refluxed for 72 h, and, following work-up, **4** was isolated as a yellow oil, which was purified *via* column chromatography (eluent: *n*-hexane/EtOAc, 2:1 v/v) ($R_f = 0.45$). Yield: 0.51 g (75%). ^1H NMR (200 MHz, CDCl_3) δ (ppm): 1.21–1.30 (m, 5H, ethyl CH_3 and hexyl CH_2) 1.44 (s, 27H, ^tBu CH_3), 1.56–1.70 (m, 4H, hexyl

CH_2), 2.29 (t, 2H, $J = 7.4$ Hz, hexyl CH_2), 2.43–2.69 (m, 6H, hexyl CH_2 and cyclen ring CH_2), 3.17–3.59 (m, 12H, cyclen ring CH_2), 4.12 (q, 2H, $J = 7.1$ Hz, ethyl CH_2). ^{13}C NMR (50 MHz, $CDCl_3$) δ (ppm): 14.5 (ethyl CH_3), 21.3 (hexyl CH_2), 23.7 (hexyl CH_2), 24.9 (hexyl CH_2), 28.7 (tBu CH_3), 34.3 (hexyl CH_2), 47.83, 48.2, 48.4, 50.3, 52.6, 53.8 (cyclen ring CH_2), 55.2 (hexyl CH_3), 60.5 (ethyl CH_2), 79.6 (tBu C), 155.6, 155.9, 156.3 (Boc group $C=O$), 173.8 (ester $C=O$). IR (cm^{-1}): 3373br w, 2977s, 2935s, 1736s, 1690s, 1463s, 1416s, 1392s, 1366s, 1251s, 1167s, 1032m, 978w, 860w, 757m. ESI-MS (m/z): 615.4 $[M+H]^+$.

1-(2-Carboxyethyl)-4,7,10-tris(tert-butoxycarbonyl)-1,4,7,10-tetraazacyclododecane (5).

Compound **2** (0.75 g, 1.3 mmol) was added to a solution of 1 M NaOH/ EtOH (20 mL, 1:1 v/v) and the reaction mixture stirred at room temperature for 4–6 h. The solvent was then removed under reduced pressure, the residue redissolved in 10% citric acid solution and the pH adjusted to 5. The product was extracted into EtOAc (2 \times 30 mL), the combined organic layers dried over Na_2SO_4 and filtered, and the solvent then removed under reduced pressure. Compound **5** was obtained as a yellow oil. Yield: 0.62 g (88%). 1H NMR (500 MHz, $CDCl_3$) δ (ppm): 1.44 (s, 27H, tBu CH_3), 2.38–2.42 (m, 4H, cyclen ring CH_2), 2.87–2.96 (m, 8H, cyclen ring CH_2), 3.24–3.33 (m, 4H, cyclen CH_2), 3.51 (s, 2H, acetate CH_2). ^{13}C NMR (125 MHz, $CDCl_3$) δ (ppm): 28.5 (tBu CH_3), 47.4, 49.9, 51.5, 51.9 (cyclen CH_2), 54.0 (acetate CH_2), 79.9 (tBu C), 155.5, 156.1 (Boc group $C=O$), 173.4 ($COOH$). IR (cm^{-1}): 3491br w, 2974s, 2931s, 1672s, 1460m, 1414s, 1364s, 1247s, 1152s, 1031m, 975m, 886m, 812m, 673w. ESI-MS (m/z): 531.3 $[M+H]^+$, 553.3 $[M+Na]^+$.

1-(4-Carboxybutyl)-4,7,10-tris(tert-butoxycarbonyl)-1,4,7,10-tetraazacyclododecane (6).

Compound **6** was synthesised from **3** (0.52 g, 0.84 mmol) following the method described for compound **5**, and was obtained as yellow oil. Yield: 0.46 g (93%). 1H NMR (500 MHz, $CDCl_3$) δ (ppm): 1.33 (s, 27H, tBu CH_3), 1.75–1.85 (m, 2H, butyl CH_2), 2.42 (t, 2H, $J = 7.5$ Hz, butyl CH_2), 2.34 (t, 2H, $J = 7.5$ Hz, butyl CH_2), 2.51–2.58 (m, 4H, cyclen ring CH_2), 3.21–3.31 (m, 8H, cyclen ring CH_2), 3.40–3.48 (m, 4H, cyclen ring CH_2). ^{13}C NMR (125 MHz, $CDCl_3$) δ (ppm): 19.1(butyl CH_2),

28.8 (^tBu CH₃), 32.2 (butyl CH₂), 47.9, 48.5, 50.0, 50.4 51.5, 52.1 (cyclen CH₂), 55.7 (butyl CH₂), 80.0 (^tBu C), 15.7, 156.2 (Boc group C=O), 177.0 (COOH). IR (cm⁻¹): 3312br w, 2975s, 2932s, 1678s, 1463s, 1416s, 1367s, 1251s, 1163s, 974w, 910w, 859w, 757s, 632s. ESI-MS (*m/z*): 559.4 [M+H]⁺, 581.4 [M+Na]⁺.

1-(6-Carboxyhexyl)-4,7,10-tris(tert-butoxycarbonyl)-1,4,7,10-tetraazacyclododecane (7).

Compound **7** was synthesised from **4** (0.60 g, 0.97 mmol) following the method described for compound **5**, and obtained as a yellow oil. Yield: 0.41 g (89%). ¹H NMR (500 MHz, CDCl₃) δ (ppm): 1.32 (m, 2H, hexyl CH₂), 1.44 (s, 27H, ^tBu CH₃), 1.63 (m, 2H, hexyl CH₂), 2.29 (t, 2H, *J* = 7.0 Hz, hexyl CH₂), 2.50–2.71 (m, 4H, cyclen ring CH₂), 2.77–2.89 (m, 2H, hexyl CH₂), 3.2–3.43 (m, 8H, cyclen ring CH₂), 3.50–3.67 (m, 4H, cyclen ring CH₂). ¹³C NMR (125 MHz, CDCl₃) δ (ppm): 24.1 (hexyl CH₂), 25.8 (hexyl CH₂), 27.9 (hexyl CH₂), 29.0 (^tBu CH₃), 35.2 (hexyl CH₂), 47.5, 48.4, 51.2, 52.8, 53.9, 55.6 (cyclen ring CH₂), 58.6 (hexyl CH₂), 79.6 (^tBu C), 156.5 (Boc group C=O), 178.2 (COOH). IR (cm⁻¹): 3460br w, 2974s, 2932s, 1680s, 1459m, 1412s, 1364s, 1247s, 1152s, 976w, 858w, 772m, 639w. ESI-MS (*m/z*): 587.4 [M+H]⁺ 609.3 [M+Na]⁺.

1-{2-[5'-(N-Boc-protected neomycin B)carboxamido]ethyl}-4,7,10-tris(tert-butoxycarbonyl)-1,4,7,10-triazacyclododecane (9). Compound **5** (0.090 g, 0.16 mmol), HBTU (0.172 g, 0.33 mmol), HOBT (0.045 g, 0.33mmol) and DIPEA (0.043 g, 0.33 mmol) were added to dry CH₂Cl₂ (10 mL). The solution was stirred for 30 min before the addition of the **8** (0.200 g, 0.16 mmol). The solution was stirred at room temperature for 20 h, after which the solvent was removed under reduced pressure. The crude product was purified by column chromatography (eluent: EtOAc) (R_f = 0.6), to give **9** as a white solid. Yield: 0.24 g (82%). ¹H NMR (500 MHz, MeOD) δ (ppm): 1.45 (m, 81H, ^tBu CH₃), 2.01 (m, 2H), 2.41 (s, 1H), 2.80–3.03 (m, 8H, cyclen CH₂), 3.17–3.61 (m, 24H), 3.74 (br s, 2H), 3.74 (s, 2H), 3.89 (m, 2H), 4.10 (m, 2H), 4.57 (s, 1H), 5.07 (s, 1H), 5.40 (s, 1H). ¹³C NMR (125 MHz, MeOD) δ (ppm): 28.1, 35.9, 41.2, 42.2, 42.9, 50.5, 50.7, 53.5, 53.9, 54.4, 55.7, 59.4, 62.3, 70.9, 71.5, 73.5, 75.1, 76.8, 79.2, 79.5, 79.9, 80.6, 82.9, 85.9, 86.7, 109.8, 113.9, 156.1, 156.9, 157.2, 157.4, 157.6, 170.5. IR

(cm^{-1}): 3422 br s, 2979m, 2531m, 2476w, 2373w, 2345w, 2105w, 1686s, 1522s, 1474m, 1458m, 1420m, 1394m, 1368s, 1275w, 1252m, 1169s, 1045m, 946w, 916w, 850m, 777w. ESI-MS (m/z): 1727.9 $[\text{M}+\text{H}]^+$.

1-{4-[5'-(*N*-Boc-protected neomycin B)carboxamido]butyl}-4,7,10-tris(*tert*-butoxycarbonyl)-1,4,7,10-triazacyclododecane (**10**). Compound **10** was synthesised from **6** (0.187 g, 0.34 mmol) and **8** (0.406 g, 0.34 mmol) following the method described for **9**. The crude product was purified by column chromatography (eluent: EtOAc) ($R_f = 0.59$). Yield: 0.44 g (75%). ^1H NMR (500 MHz, MeOD) δ (ppm): 1.26 (m, 2H, butyl CH_2), 1.42 (m, 81H, ^tBu CH_3), 1.81 (t, $J=7$ Hz, 2H, butyl CH_2), 1.96 (s, 1H), 2.01 (s, 1H), 2.28–2.35 (m, 8H, cyclen CH_2), 2.67–2.73 (m, 10H, cyclen CH_2), 2.67–2.73 (m, 10H), 3.19 (t, $J = 9.0$ Hz, 2H), 3.29–3.61 (m, 16H), 3.75 (br s, 1H), 3.90–4.11 (m, 2H), 4.28 (s, 1H), 5.06 (s, 1H), 5.39 (s, 1H). ^{13}C NMR (125 MHz, MeOD) δ (ppm): 24.9, 28.3, 34.8, 35.9, 41.4, 42.4, 42.9, 50.7, 50.9, 53.7, 53.9, 54.6, 55.9, 59.7, 59.9, 62.6, 71.3, 71.8, 73.9, 75.5, 77.1, 79.7, 79.9, 80.1, 80.9, 83.1, 86.0, 86.9, 110.1, 114.2, 156.3, 156.9, 157.4, 157.6, 157.9, 170.8. ESI-MS (m/z): 1754.5 $[\text{M}+\text{H}]^+$

1-{6-[5'-(*N*-Boc-protected neomycin B)carboxamido]hexyl}-4,7,10-tris(*tert*-butoxycarbonyl)-1,4,7,10-triazacyclododecane (**11**). Compound **11** was synthesised from **7** (0.300 g, 0.50 mmol) and **8** (0.608 g, 0.50 mmol) following the method described for **9**. The crude product was purified by column chromatography (eluent: EtOAc) ($R_f = 0.57$). Yield: 0.66 mg (72%). ^1H NMR (500 MHz, MeOD) δ (ppm): 1.28 (t, $J = 7.0$ Hz, 2H, hexyl CH_2), 1.31–1.54 (m, 87H, ^tBu CH_3 and hexyl CH_2), 1.69 (m, 2H, hexyl CH_2), 2.33–2.39 (m, 4H, hexyl CH_2), 2.69 (br s, 6H, cyclen CH_2), 3.18–3.59 (m, 18H), 3.76 (m, 6H), 4.07–4.12 (m, 3H), 5.01 (s, 1H), 5.48 (s, 2H), 6.23 (d, $J = 10$ Hz, 2H). ^{13}C -NMR (125MHz, MeOD) δ (ppm): 25.5, 26.5, 27.8, 28.4, 35.8, 36.8, 41.3, 42.1, 42.8, 50.3, 50.9, 53.6, 53.8, 54.3, 55.7, 59.5, 59.7, 59.9, 62.5, 71.0, 71.7, 73.8, 75.4, 76.9, 79.6, 79.8, 80.0, 80.6, 82.9, 86.0, 86.5, 110.0, 114.0, 156.1, 156.7, 157.2, 157.5, 157.8, 170.6. IR (cm^{-1}): 3422br s, 2979s, 2934s, 2508w, 1692s, 1522s,

1480w, 1458w, 1419m, 1393w, 1368s, 1278m, 1252s, 1168s, 1044m, 852m, 776w. ESI-MS (m/z): 1784.0 $[M+H]^+$.

1-{2-[5'-(Neomycin B)carboxamido]ethyl}-1,4,7,10-triazacyclododecane (C1). Compound **9** (0.355 g, 0.21 mmol) was dissolved in TFA/CH₂Cl₂ (10 mL, 1:1 v/v) and the solution was stirred at room temperature for 5 h. The solvent was then removed under reduced pressure, and the crude residue purified by preparatory HPLC (Jupiter C18 Prep Column (5 μ m, 300 Å, 4.6 \times 250 mm), monitored at 210 nm) using a linear gradient from 100% H₂O (0.1% TFA) to 85% H₂O: 15% CH₃CN over 40 min. The product eluted between 19–23 min and was isolated as a white solid (TFA salt) following removal of the solvent. Yield: 0.150 g (39%). ¹H NMR (500 MHz, D₂O) δ (ppm): 1.18 (d, J = 7.0 Hz, 1H), 1.75 (d, J = 12.5 Hz, 1H), 2.35 (d, J = 8.5 Hz, 1H), 2.84 (br s, 6H), 3.02 (m, 8H), 3.15–3.52 (m, 12H), 3.59 (t, J = 10 Hz, 2H), 3.70 (br s, 1H), 3.77–3.89 (m, 4H), 3.97 (t, J = 9.5 Hz, 1H), 4.03–4.09 (m, 2H), 4.18–4.22 (m, 3H), 5.15 (s, 1H), 5.25 (s, 1H), 5.84 (d, J = 4.0 Hz, 1H). ¹³C NMR (125 MHz, D₂O) δ (ppm): 27.9, 40.1, 40.5, 41.9, 42.5, 44.5, 48.6, 49.3, 49.7, 50.9, 53.1, 55.2, 67.5, 67.6, 68.2, 70.2, 72.2, 73.0, 75.5, 77.0, 80.0, 84.6, 94.9, 95.5, 109.6, 112.0, 114.9, 117.8, 120.7, 173.5. IR (cm⁻¹): 3313m, 3088m, 2874m, 2358w, 2338w, 2148w, 2039w, 2002w, 1669s, 1636w, 1559m, 1540m, 1522m, 1457w, 1429m, 1321w, 1183s, 1125s, 1074w, 1049w, 1014m, 837m, 798s, 722s. High-resolution ESI-MS (C₃₃H₆₇N₁₁O₁₃): Calcd. 826.9403 $[M+H]^+$, Found 826.4998. Microanalysis: Found (%): C, 30.93; H, 4.69; N, 7.99; F, 24.18. Calcd. for C₃₃H₆₇N₁₁O₁₃·8TFA·8H₂O (%): C, 32.27; H, 4.87; N, 8.19; F, 24.22.

1-{4-[5'-(Neomycin B)carboxamido]ethyl}-1,4,7,10-triazacyclododecane (C2). Compound **C2** was synthesised from compound **10** (0.411 g, 0.23 mmol) following the method described for preparation of **C1**. Yield: 0.156 g (35%). ¹H NMR (500 MHz, D₂O) δ (ppm): 1.65 (br s, 2H), 1.76 (s, 1H), 2.17 (t, J = 7.5 Hz, 4H), 2.34 (br s, 2H), 2.55 (s, 2H), 2.79 (br s, 6H), 2.98 (br s, 6H), 3.15–3.37 (m, 8H), 3.41–3.45 (m, 3H), 3.58 (s, 1H), 3.68 (s, 1H), 3.69 (s, 1H), 3.77–3.88 (m, 3H), 3.97 (t, J = 9.0

Hz, 2H), 4.08 (s, 2H), 4.15 (m, 2H), 4.22 (t, $J = 4.5$ Hz, 1H), 5.14 (s, 1H), 5.25 (s, 1H), 5.82 (s, 1H). ^{13}C NMR (125 MHz, D_2O) δ (ppm): 19.3, 27.9, 33.0, 40.1, 40.5, 41.6, 41.9, 44.1, 47.7, 48.5, 49.6, 50.9, 51.6, 53.2, 67.4, 67.6, 68.1, 69.8, 70.2, 70.5, 72.3, 73.3, 75.2, 77.4, 80.4, 84.9, 94.9, 95.7, 109.5, 176.3. IR (neat), (cm^{-1}): 3549w, 3348w, 3083m, 2879m, 2731m, 2543m, 1670s, 1541w, 1528w, 1429w, 1281w, 1187s, 1127s, 1074w, 1050w, 1017w, 837m, 798m, 766w, 722s. High-resolution ESI-MS ($\text{C}_{35}\text{H}_{71}\text{N}_{11}\text{O}_{13}$): Calcd. 854.0055 $[\text{M}+\text{H}]^+$, Found 854.5289. Microanalysis: Found (%): C, 32.21; H, 4.58; N, 8.05; F, 28.97. Calcd. for $\text{C}_{35}\text{H}_{71}\text{N}_{11}\text{O}_{13}\cdot 10\text{TFA}$ (%): C, 32.54; H, 4.22; N, 7.59; F, 28.07.

1-{6-[5'-(Neomycin B)carboxamido]hexyl}-1,4,7,10-triazacyclododecane (C3). Compound **C3** was synthesised from **11** (0.650 g, 0.36 mmol) following the method described for compound **C1**. Yield: 0.28 g (40%). ^1H NMR (500 MHz, D_2O) δ (ppm): 1.15 (s, 2H), 1.23 (s, 1H), 1.42–1.46 (m, 3H), 1.56 (s, 1H), 1.74–1.78 (m, 2H), 2.14 (t, $J = 7$ Hz, 2H), 2.33–2.37 (m, 1H), 2.56 (s, 1H), 2.67 (br s, 2H), 2.91 (d, $J = 10.5$ Hz, 12H), 3.18–3.45 (m, 12H), 3.584 (t, $J = 10$ Hz, 2H), 3.69 (s, 1H), 3.77–3.89 (m, 3H), 3.97 (t, $J = 9$ Hz, 1H), 4.08–4.16 (m, 4H), 4.23 (m, 1H), 5.14 (s, 1H), 5.25 (s, 1H), 5.82 (1H). ^{13}C NMR (125 MHz, D_2O) δ (ppm): 22.8, 25.3, 26.1, 28.4, 35.8, 40.1, 40.5, 41.4, 41.8, 42.4, 43.6, 48.6, 48.8, 49.7, 50.9, 52.5, 53.3, 67.4, 67.6, 68.3, 69.7, 70.2, 70.5, 72.4, 73.4, 75.8, 77.5, 80.5, 85.0, 95.0, 95.8, 109.4, 177.4 IR (neat), (cm^{-1}): 3372m, 3280m, 2925m, 2876m, 2362w, 2150w, 1670s, 1637w, 1533w, 1459w, 1457w, 1429w, 1183s, 1125s, 1074w, 1050w, 1015w, 837m, 798m, 766w, 722s. High-resolution ESI-MS ($\text{C}_{37}\text{H}_{75}\text{N}_{11}\text{O}_{13}$): Calcd. 882.059 $[\text{M}+\text{H}]^+$, Found 882.5649. Microanalysis: Found (%): C, 33.49; H, 4.76; N, 8.11; F, 24.69. Calcd. for $\text{C}_{37}\text{H}_{75}\text{N}_{11}\text{O}_{13}\cdot 8\text{TFA}\cdot 5\text{H}_2\text{O}$ (%): C, 33.78; H, 4.97; N, 8.18; F, 24.2.

Aminoglycoside binding studies. Binding studies were conducted using 1 μM solutions of Dy547 A-site RNA in 20 mM calcodylate buffer (pH 7.0, 100 mM, NaCl, 0.5 mM EDTA). The Dy547 A-site was annealed by heating solutions to 75 $^\circ\text{C}$ for 5 min, cooling to room temperature over 2 h, and then to 0 $^\circ\text{C}$ for 30 min. They were then allowed to warm back to room temperature. For experiments

involving the Zn(II) complexes of the conjugates, EDTA was removed from the buffer. These complexes were prepared by combining **C1–C3** with Zn(II) in a 1:1 molar ratio using a stock Zn(II) solution made by dissolving a commercial standard solution of ZnCl₂ in water.

The FRET-based displacement-style binding experiments were carried out at 21 °C on a Horiba Fluoromax-4 luminescence spectrometer, using excitation and emission slit widths of 9 nm and with background correction (spectrum of buffer was subtracted from each sample). In a typical run, 125 μL of Dy547 A site solution (1 μM) was placed in a 0.5 mL quartz fluorescence cell with a path length of 1.0 cm (Hellma GmbH & Co KG, Müllheim, Germany). To this, 0.66 μL of a 94.4 μM stock solution of Kanamycin A-coumarin (**12**) or neomycin B-coumarin (**13**) was then added to reach a final concentration of 0.5 μM for **12** or **13**, in solution. The coumarin-Dy547 FRET system was excited at 400 nm and changes in emission at 561 nm were monitored after the addition of increasing amounts (1 μL aliquots of 10 mM stock solution) of a conjugate or its Zn(II) complex, to assess the degree of displacement of kanamycin- and neomycin-coumarin from Dy547 A-site. The OriginPro 8 software was used to calculate IC₅₀ values by fitting a dose response curve to the fractional fluorescence saturation (F_s) plotted against the log of aminoglycoside (AG) concentration (eq 1).

$$F_s = F_0 + (F_\infty [AG]^n) / ([IC_{50}]^n + [AG]^n) \quad (1)$$

F_0 and F_∞ are the fluorescence intensity in the absence of aminoglycoside or at saturation, respectively, and n is the Hill coefficient or degree of cooperativity associated with binding. Error estimates were generated from three sets of measurements.

Acknowledgment

This work was supported by funding from the Australian Research Council through a Future Fellowship to BG (FT130100838), a Discovery Grant to LS, BG and YT (DP1094100) as well as a Discovery Outstanding Researcher Award and Discovery Grant to LS (DP130100816).

Supporting Information Available

Representative example of a FRET titration graph (Figure S1); typical dose response curve (Figure S2); pH-dependence of the affinities of neomycin B and conjugate **C1** for the A-site (Figures S3–S4).

References

1. Y. Tor, *ChemBioChem*, 2003, **4**, 998-1007.
2. K. Michael and Y. Tor, *Chem. Eur. J.*, 1998, **4**, 2091-2098 and references therein.
3. H. Wang and Y. Tor, *Angew. Chem. Int. Ed.*, 1998, **37**, 109-111.
4. R. Maviglia, R. Nestorini and M. Pennisi, *Curr. Drug Targets*, 2009, **10**, 895-905.
5. P. Dozzo and H. E. Moser, *Expert Opin. Ther. Pat.*, 2010, **20**, 1321-1341.
6. L. Yang and X. S. Ye, *Curr. Top. Med. Chem.*, 2010, **10**, 1898-1826.
7. M. Bassetti, F. Ginocchio, M. Mikulska, L. Taramasso and D. R. Giacobbe, *Expert Rev. Anti Infect. Ther.*, 2011, **9**, 909-922.
8. R.-B. Yan, *Bioorg. Med. Chem.*, 2011, **19**, 30-40.
9. M. Bassetti, M. Merelli, C. Temperoni and A. Astilean, *Ann. Clin. Microbiol. Antimicrob.*, 2013, **12**, 22.
10. J. Jackson, C. Chen and K. Buising, *Curr. Opin. Infect. Dis.*, 2013, **26**, 516-525.
11. J. L. Houghton, K. D. Green, W. Chen and S. Garneau-Tsodikova, *ChemBioChem*, 2010, **11**, 880-902.
12. F. Zhao, Q. Zhao, K. F. Blount, Q. Han, Y. Tor and T. Hermann, *Angew. Chem. Int. Ed.*, 2005, **44**, 5329-5334.
13. Y. Tor, *Angew. Chem. Int. Ed.*, 1999, **38**, 1579-1582.
14. R. Schroeder, C. Waldsich and H. Wank, *EMBO J.*, 2000, **19**, 1-9.
15. J. Gallego and G. Varani, *Acc. Chem. Res.*, 2001, **34**, 836-843.
16. V. K. Tam, D. Kwong and Y. Tor, *J. Am. Chem. Soc.*, 2007, **129**, 3257-3266.
17. S. R. Kirk, N. W. Luedtke and Y. Tor, *J. Am. Chem. Soc.*, 2000, **122**, 980 - 981.
18. K. F. Blount, F. Zhao, T. Hermann and Y. Tor, *J. Am. Chem. Soc.*, 2005, **127**, 9818-9829.
19. T. D. Bradrick and J. P. Marino, *RNA*, 2004, **10**, 1459-1468.
20. K. F. Blount and Y. Tor, *ChemBioChem*, 2006, **7**, 1612-1621.
21. S. G. Srivatsan and Y. Tor, *Tetrahedron*, 2007, **63**, 3601-3607.
22. M. Hainrichson, I. Nudelman and T. Baasov, *Org. Biomol. Chem.*, 2008, **6**, 227-239.
23. R. J. Fair, M. E. Hensler, W. Thienphrapa, Q. N. Dam, V. Nizet and Y. Tor, *ChemMedChem*, 2012, **7**, 1237-1244.
24. J. Lee, M. Kwon, K. H. Lee, S. Jeong, S. Hyun, K. J. Shin and J. Yu, *J. Am. Chem. Soc.*, 2004, **126**, 1956-1957.
25. D.-R. Ahn and J. Yu, *Bioorg. Med. Chem.*, 2005, **13**, 1177-1183.
26. H. Wang and Y. Tor, *J. Am. Chem. Soc.*, 1997, **119**, 8734-8735.
27. F. Walter, Q. Vicens and E. Westhof, *Curr. Opin. Chem. Biol.*, 1999, **3**, 694-704.
28. T. Joshi, B. Graham and L. Spiccia, *Acc. Chem. Res.*, 2015, **48**, 2366-2379.
29. E. Kimura, S. Aoki, T. Koike and M. Shiro, *J. Am. Chem. Soc.*, 1997, **119**, 3068-3076.

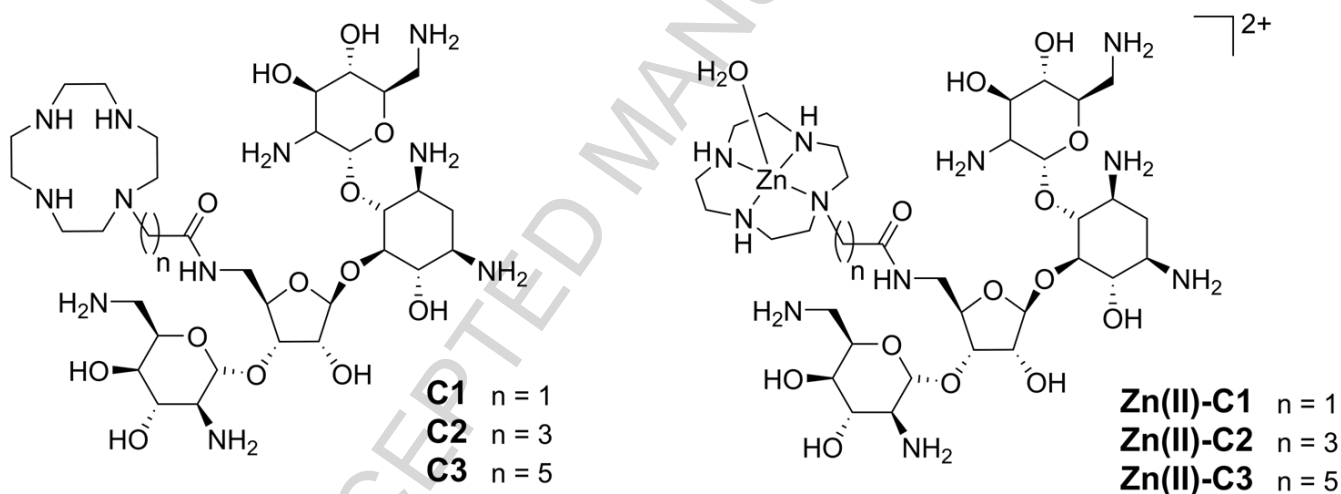
30. S. Aoki and E. Kimura, *J. Am. Chem. Soc.*, 2000, **122**, 4542-4548.
31. R. Reichenbach-Klinke and B. König, *J. Chem. Soc., Dalton Trans.*, 2002, 121-130.
32. Y. Xie, A. V. Dix and Y. Tor, *J. Am. Chem. Soc.*, 2009, **131**, 17605-17614.
33. Y. Xie, A. V. Dix and Y. Tor, *Chem. Commun.*, 2010, **46**, 5542-5544.
34. M. J. Belousoff, B. Graham, L. Spiccia and Y. Tor, *Org. Biomol. Chem.*, 2009, **7**, 30-33.
35. M. Briellmann, S. Kaderli, C. J. Meyer and A. D. Zuberbühler, *Helv. Chim. Acta*, 1987, **70**, 680-689.
36. M. Kodama and E. Kimura, *J. Chem. Soc., Dalton Trans.*, 1980, 327-333.
37. M. Belousoff, G. Gasser, B. Graham, Y. Tor and L. Spiccia, *J. Biol. Inorg. Chem.*, 2009, **14**, 287-300.

Highlights

- Three new neomycin B derivatives were prepared which feature an alkyl chain-linked 1,4,7,10-tetraazacyclododecane (cyclen) macrocycle.

- Binding affinity of neomycin B-cyclen conjugates and their zinc(II) complexes for A-site RNA was examined by FRET-based measurements.
- Conjugates bind to the A-site with higher affinities than neomycin B due to their higher overall positive charge, arising from protonated cyclen ring.
- The Zn(II) complexes bind more strongly due to coordinative (and/or electrostatic) interactions between cationic Zn(II)-cyclen moiety and phosphates or deprotonated uracil bases.

Figure for TOC:



Synopsis:

Three new derivatives of the aminoglycoside antibiotic neomycin B, incorporating the 1,4,7,10-tetraazacyclododecane macrocycle, are reported together with an examination of the ability of these compounds and their zinc(II) complexes to bind to the prokaryotic ribosomal A-site RNA via FRET-based measurements.